http://ansinet.com/itj

ITJ

ISSN 1812-5638

INFORMATION TECHNOLOGY JOURNAL

ANSInet
Asian Network for Scientific Information
308 Lasani Town, Sargodha Road, Faisalabad - Pakistan

Information Technology Journal 13 (14): 2229-2239, 2014
ISSN 1812-5638 / DOI: 10.3923/itj.2014.2229.2239

Performance Analysis of CRNs Based on Joint Spatial and Temporal Spectrum Sharing[1]

Peipei Chen, Qinyu Zhang, Weiqiang Wu and Yalin Zhang
Department of Electronic and Information Engineering,
Harbin Institute of Technology, Shenzhen Graduate School, Shenzhen, China

Abstract: In this study, we propose a joint spectrum sensing scheme for Cognitive Radio Networks (CRNs) based on joint spatial and temporal spectrum sharing under Primary User (PU) inference constraint. Compared with temporal spectrum sharing and spatial spectrum sharing, joint spatial and temporal spectrum sharing can exploit more spectrum holes and thereby improve the throughput of secondary system. In the proposed sensing scheme, the mechanism for deriving spatial spectrum hole is given as MIFTP-JSTS (MIFTP based on joint spatial and temporal sensing). The relationship between the spatial and temporal spectrum sensing is revealed. For CRNs with specific periodical spectrum sensing, tradeoff exists between the performances of spectrum sensing and spectrum sharing. An optimization problem is formulated to optimize the performance of spectrum sharing in CRNs and the optimal sensing duration can be derived. Through simulation results and analysis, advantage regions exist for CRNs based on joint spatial and temporal spectrum sharing.

Key words: Joint spatial and temporal spectrum sharing, optimal sensing duration, advantage region

INTRODUCTION

In wireless communication, spectrum is the indispensable resource for transmission. Static spectrum allocation mechanism has been utilized for a long time and works well for many years. Most of the spectrum has been allocated as licensed spectrum to licensed system (NTIA, 2003). No more spectrum can be allocated to the emerging wireless services and wireless techniques. Spectrum is becoming a scarce resource. However, measurements and surveys on spectrum utilization (FCC, 2002; Islam *et al*., 2008) show that most of the licensed spectrum is highly underutilized. Cognitive Radio (CR) is a promising technology to solve the contradictions, in which Secondary Users (SUs) can share the spectrum with the Primary Users (PUs) by opportunistically access the spectrum holes (Mitola III, 1999). With respect to a frequency channel of interest, spatial spectrum hole refers to the Maximal Interference-free Transmit Power (MIFTP) for Secondary User (SU) when PU's presence is sensed, whereas, temporal spectrum hole refers to a period of time in which SU can transmit when no PU is sensed.

Spatial spectrum sharing and temporal spectrum sharing have been attracted a lot of attentions, respectively (Ghasemi and Sousa, 2008; Zou *et al*., 2010; Taricco, 2011; Sahai *et al*., 2006; Mark and Nasif, 2009; Min *et al*., 2010). Joint spatial and temporal spectrum sharing mechanism can exploit more spectrum holes and improve the throughput of CRNs. However, it is seldom investigated. Do and Mark (2010) have considered the joint spatial and temporal spectrum sharing but only the interference caused by temporal spectrum sharing is included. PU may experience harmful interference caused by spatial spectrum sharing which is not allowable in CRNs. The spatial spectrum hole is derived based on spatial spectrum sensing scheme which is proposed by Mark and Nasif (2009). For simplicity, we denote the spatial spectrum hole deriving scheme proposed by Mark and Nasif (2009) as MIFTP-PS. As we know, the working mode of Primary Transmitter (PT) has both ON and OFF state. The working mode of PT in MIFTP-PS scheme is assumed always in ON state which is inconsistent with the reality and may cause unacceptable interference to PUs.

In this study, we study the performance of joint spatial and temporal spectrum sharing mechanism in CRNs. Firstly, we propose a joint spectrum sensing scheme with PU interference constraint. Secondly, we focus on how to achieve efficient joint spatial and temporal sensing to maximize the throughput of secondary system.

Corresponding Author: Peipei Chen, Department of Electronic and Information Engineering,
Harbin Institute of Technology, Shenzhen Graduate School, Shenzhen, China

[1]**Foundation Items:** China Postdoctoral Science Foundation (2013M540289)

According to the primary service characteristic, PT alternates between ON and OFF states. By using the temporal sensing algorithm, the PT's activity state can be acquired. We use cooperative energy detection here (Zou *et al*., 2010). Given the temporal sensing algorithm and received Signal to Noise Ratio (SNR), we study the relationship between temporal sensing performance (including false alarm probability P_f and detection probability P_d) and sensing duration. When no PT is sensed, SU can transmit with its maximum power. When sensing result indicates PT is present, the spatial spectrum hole would constrain the SU's transmit power. Here PT's location, transmit power and SU's location are assumed available (Chen *et al*., 2013). The real-time activity pattern of PT still needs to be sensed by temporal sensing. The PU interference constraint is considered in our study, in which both the interference caused by temporal and spatial spectrum sharing are included. We derive the relationship between spatial spectrum hole and temporal spectrum hole by PU interference model. For simplicity, we denote the sensing scheme for spatial spectrum hole in CRNs based on joint spatial and temporal spectrum sharing as MIFTP-JSTS.

To our knowledge, the performance of temporal sensing is measured by two key factors: probability of detection errors and sensing time (Zou *et al*., 2010). The main idea of the traditional way to design a sensing strategy is to protect PU, i.e., to maximize the detection probability under the constraint of false alarm probability (Kay, 1998). Another criterion is to minimize the false alarm probability under the constraint of detection probability for maximizing the temporal spectrum sharing in CRNs (Liang *et al*., 2008). Zou *et al*. (2010) proposed the design methodology of minimizing the required sensing time, subject to a constraint of the detection errors. In this context, we formulate an optimization problem to maximize the throughput of secondary system. The optimal sensing duration can be achieved which yields the maximum throughput of secondary system. With the analysis and simulation results, we observe that the joint spatial and temporal spectrum sharing outperforms the temporal and spatial spectrum sharing in terms of the secondary system throughput in the specific advantage region.

SYSTEM MODEL

In CRNs, SUs periodically scan the licensed spectrum of primary system in order to find spectrum holes. As we assume that the location of PT can be obtained, the location of primary receiver can be approximately derived from the protection range of PT (Taricco, 2011). The location of Primary Receiver (PR) is in the protection range of PT. In CRNs, for satisfying the PU interference constraint, only the Worst PR Position (WPRP) needs to be considered (Mark and Nasif, 2009). The position of WPRP is identified in Fig. 1.

The interference probability of the PR at WPRP can be presented as:

$$P_{int} = \Pr\{I \geq \kappa_{max} | E\}\Pr\{E\} + \Pr\{I \geq \kappa_{max} | \bar{E}\}\Pr\{\bar{E}\} \quad (1)$$

where, $\Pr\{E\}$ and $\Pr(\bar{E})$ represent the detection probability and miss detection probability that when PT is active which can be denoted as P_d and P_m. I denotes the interference caused by Secondary Transmitter (ST)

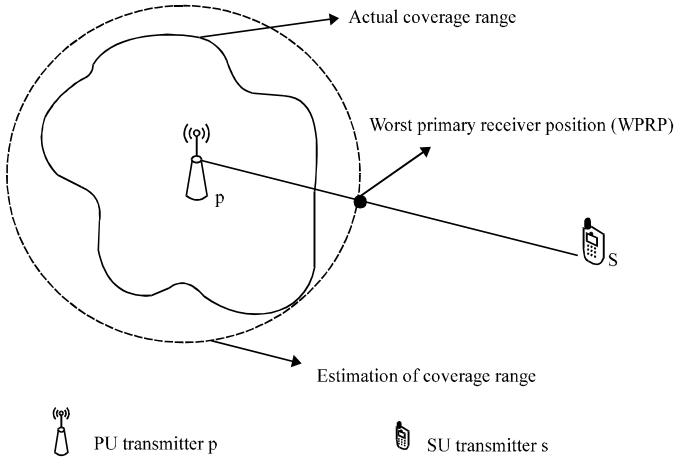

Fig. 1: Schematic diagram of MIFTP estimation

while κ_{max} denotes the specific interference threshold. $Pr\{I \geq \kappa_{max} | E\}$ and $Pr\{I \geq \kappa_{max} | \bar{E}\}$ represent the corresponding interference probability caused by ST in above two situations which can be denoted as P_{dI} and O_{mI}.

According to our previous work (Chen *et al*., 2013), the expression of P_{dI} and P_{mI} can be given as following:

$$P_{dI} = \frac{1}{2}\left[1 - erf\left(\frac{\kappa_{max} - P_{MIFTP} + g(d)}{\sigma_W\sqrt{2}}\right)\right] \quad (2)$$

$$P_{mI} = \frac{1}{2}\left[1 - erf\left(\frac{\kappa_{max} - P_{max} + g(d)}{\sigma_W\sqrt{2}}\right)\right] \quad (3)$$

where, $g(d) = 10\rho\log_{10}(d/d_0)$, d denotes the distance between ST and PR at WPRP, d_0 is the reference distance and ρ is the path loss factor, σ_W is the shadowing noise. And we can also get the expression of spatial spectrum hole P_{MIFTP}:

$$P_{MIFTP} = \kappa_{max} + g(d) + erf^{-1}\left(2\left(P_{mI} + \frac{\varsigma - P_{mI}}{P_d}\right) - 1\right)\sigma_W\sqrt{2}n \quad (4)$$

where, P_{mI}, $(1-P_d)<\varsigma$, ς represents the PU interference constraint.

It can be seen that the spatial spectrum hole based on MIFTP-JSTS scheme depends not only on the parameters including distance between ST and PT, shadowing fading in transmission, PU's tolerable interference probability but also the temporal sensing's detection probability P_d. Base on the temporal sensing result, ST s can acquire the spatial spectrum hole according to its relative distance to PT and the temporal sensing performance.

It can be observed that with P_d increasing, with PU interference constraint, the allowable interference probability during spatial spectrum sharing P_{dI} increases which means that P_{MIFTP} increases. The inner relationship between temporal and spatial sensing has not been discussed in previous research works as we know which is first studied in our study. Detection probability in temporal spectrum sensing is related with sensing duration τ (Ghasemi and Sousa, 2008). Furthermore, the relationship between the spatial spectrum hole based on MIFTP-JSTS and sensing duration can also be achieved.

COOPERATIVE TEMPORAL SPECTRUM SENSING

Hypothesis testing in cooperative temporal sensing: The temporal spectrum sensing can be modeled as a binary hypothesis testing problem, in which two hypotheses are defined separately as H_0 and H_1 corresponding to the signal absent and signal present events.

The signal acquired by the mth SU is represented as following, (m = 1, 2,…, M):

$$\begin{aligned} H_0&: X_m[n[= w_m[n] \\ H_1&: X_m[n] = S_m[n] + w_m[n] \end{aligned} \quad (5)$$

We assume that the signal $S_m[n]$ is an independent and identical distributed random process with mean zero and variance $\sigma^2_{s,m}$ and the signal is modulated by complex PSK.

Noise $w_m[n]$ are independent, identical Gaussian distributed with mean zero and variance $\sigma^2_{w,m}$. N is the sampling number, $N = \tau f_s$, τ is the sensing duration, f_s is the sampling frequency. For simplification, we assume that the noises at the sensing nodes are the same, i.e., $\sigma^2_{w,m} = \sigma^2_w$.

According to the energy detection, the test statistic can be represented as:

$$T_m = \frac{1}{N}\sum_{n=1}^{N}\left|X_m[n]\right|^2 \quad (6)$$

Under H_0, the distribution of T_m is a central Chi-square distribution with N degrees freedom while under H_1, the distribution of the T_m is a non-central Chi-square distribution with N degrees freedom. When N is large enough (N>250), according to the Central Limit Theorem (Liang *et al*., 2008), we can get:

$$T_m \sim \begin{cases} N\left(\sigma_w^2, \frac{\sigma_w^4}{N}\right) & H_0 \\ N\left(\sigma_{S,m}^2 + \sigma_w^2, \frac{2\sigma_{S,m}^2\sigma_w^2 + \sigma_w^4}{N}\right) & H_1 \end{cases} \quad (7)$$

Data fusion in cooperative temporal sensing: In temporal cooperative sensing, the fusion center/BS processes the measurements collected from all the sensing nodes and then makes the final decision.

Using data fusion, the test statistic in fusion center/BS can be represented as:

$$T = \frac{1}{\sqrt{M}}\sum_{m=1}^{M} T_m \quad (8)$$

Using the similar deduction of T_m, for large N, according to the Central Limit Theorem, we can get:

$$T \sim \begin{cases} N\left(\sigma_w^2\sqrt{M}, \frac{\sigma_w^4}{N}\right) & H_0 \\ N\left(\frac{\sigma_w^2}{\sqrt{M}}\sum_{m=1}^{M}\left(\frac{\sigma_{S,m}^2}{\sigma_w^2} + 1\right), \frac{\sigma_w^4}{N}\left(1 + \frac{2}{M}\sum_{m=1}^{M}\frac{\sigma_{S,m}^2}{\sigma_w^2}\right)\right) & H_1 \end{cases} \quad (9)$$

For simplicity, we denote $\gamma_m = \sigma^2_{S,m}/\sigma^2_w$ as the received Signal to Noise Ratio (SNR) at the mth SU.

With detection threshold η, we can get the false alarm probability and detection probability as following:

$$P_f = \Pr\{T > \eta | H_0\} = \int_\eta^{+\infty} p_0(x)dx \quad (10)$$

$$P_d = \Pr\{T > \eta | H_1\} = \int_\eta^{+\infty} p_1(x)dx \quad (11)$$

where, $p_0(x)$ and $p_1(x)$ represent the Probability Density Function (PDF) of T under hypothesis H_0 and H_1 respectively and which can be easily derived from Eq. 7.

Hence, the false alarm probability P_f and detection probability P_d can be achieved:

$$P_f = Q\left(\left(\frac{\eta}{\sigma_w^2} - \sqrt{M}\right)\sqrt{\tau f_s}\right) \quad (12)$$

$$P_d = Q\left(\left(\frac{\eta - \frac{\sigma_w^2}{\sqrt{M}}\sum_{m=1}^{M}(\gamma_m + 1)}{\sigma_w^2\sqrt{1 + \frac{2}{M}\sum_{m=1}^{M}\gamma_m}}\right)\sqrt{\tau f_s}\right) \quad (13)$$

Detection threshold value η can be eliminated by combining the above two equations and the relationship between P_d and P_f can be given as following:

$$P_d = Q\left(\frac{1}{\sqrt{\left(2\sum_{m=1}^{M}\gamma_m \Big/ M\right) + 1}}\left(Q^{-1}(\bar{P}_f) - \sqrt{\frac{\tau f_s}{M}}\sum_{m=1}^{M}\gamma_m\right)\right) \quad (14)$$

$$P_f = Q\left(\sqrt{\left(2\sum_{m=1}^{M}\gamma_m \Big/ M\right) + 1} \times Q^{-1}(\bar{P}_d) + \sqrt{\tau f_s / M}\sum_{m=1}^{M}\gamma_m\right) \quad (15)$$

where, $\bar{P}_f$ and $\bar{P}_d$ represent the target probability of false alarm and target probability of detection probability, respectively. Given $\bar{P}_f$, P_d increases as the sensing duration τ increases. Given $\bar{P}_d$, the false alarm probability P_f decreases as sensing duration τ increases correspondingly.

Relationship between spectrum sensing time and throughput: Figure 2 shows the MAC frame construction of SUs with periodically sensing capability in CRNs. Every frame consists of sensing slot with duration time of τ and transmission slot with duration time of T-τ.

According to the analysis in last section, the spatial spectrum hole increases with detection probability P_d.

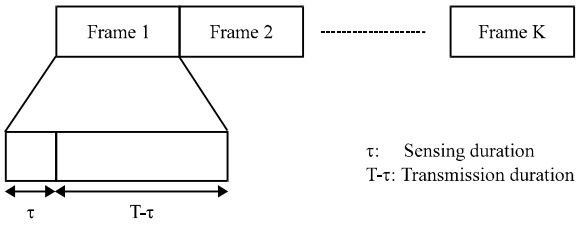

Fig. 2: Frame structure of SUs with periodical spectrum sensing in CRNs

Meanwhile, we get the conclusion that P_d is an increasing function of τ in above subsection. As a result, we can conclude that P_{MIFTP} increases with τ.

With given false alarm probability, longer sensing duration contributes to larger spatial spectrum hole. With given detection probability, longer sensing duration contributes to smaller false alarm probability and more chances for SU to use temporal spectrum hole. However, transmission time for SU become smaller. As a result, we can conclude that there exists a tradeoff between sensing duration and spectrum sharing in CRNs based on joint spatial and temporal spectrum sensing.

ACHIEVABLE THROUGHPUT OF SECONDARY SYSTEM

In this section, we present the achievable throughput of secondary system. For a given frequency channel of interest, four situations exist when the secondary system use the joint spatial and temporal spectrum sharing mechanism. The probability for hypothesis H_0 is denoted as $P(H_0)$, whereas, the probability for hypothesis H_1 is denoted as $P(H_1)$.

Situation 1: The PT signal is present and successfully detected by SUs in cooperative temporal sensing. The probability for this situation can be presented as $P(H_1)P_d$. Spatial spectrum hole can be utilized when $P_{MIFTP}>0$ and transmission power of ST s is P_{MIFTP}. In this situation, the achievable throughput of the secondary link can be represented as:

$$C_{ST1} = \frac{T-\tau}{T} B \cdot E\left\{\log_2\left(1 + \frac{P_{MIFTP}(d_0/D_{ss})^n e^X}{P_p(d_0/d_{ps})^n e^Y + N_0 B}\right)\right\} \quad (16)$$

where, $X \sim N(0, \sigma_X)$ and $Y \sim N(0, \sigma_Y)$ denote shadowing fading, $E[\cdot]$ denotes the expectation that with respected to the shadowing fading. D_{ss} represents the distance of SU transmitter-receiver link and d_{ps} represents the distance of PT-SR link.

Situation 2: The PT signal is presents and missed detected by SUs in cooperative temporal sensing. The probability for this scenario can be presented as $P(H_1)(1-P_d)$. Transmission power of ST S is P_{max}. In this situation, the achievable throughput of the secondary link is:

$$C_{ST2} = \frac{T-\tau}{T} B \cdot E\left\{\log_2\left(1+\frac{P_{max}\left(d_0/D_{ss}\right)^n e^X}{P_p\left(d_0/d_{ps}\right)^n e^Y + N_0 B}\right)\right\} \quad (17)$$

Situation 3: The PT signal is absent but SUs in cooperative sensing falsely judge that PT signal is present. The probability for this situation is $P(H_1)P_f$. Instead of the temporal spectrum hole, spatial spectrum hole can be utilized when $P_{MIFTP}>0$ and transmission power of STs is P_{MIFTP}. In this situation, the achievable throughput of the secondary link is:

$$C_{ST3} = \frac{T-\tau}{T} B \cdot E\left\{\log_2\left(1+\frac{P_{MIFTP}\left(d_0/D_{ss}\right)^n e^X}{N_0 B}\right)\right\} \quad (18)$$

Scenario 4: The PT signal is absent and SUs in cooperative sensing successfully detect the PT signal. The probability for this scenario is $P(H_1)(1-P_f)$. Temporal spectrum hole can be utilized and transmission power of ST s is P_{max}. In this situation, the achievable throughput of the secondary link is:

$$C_{ST4} = \frac{T-\tau}{T} B \cdot E\left\{\log_2\left(1+\frac{P_{max}\left(d_0/D_{ss}\right) e^X}{N_0 B}\right)\right\} \quad (19)$$

In summary, we can achieve the formulation of the average throughput for secondary as Eq. 20:

$$C_{ST} = C_{ST1}P(H_1)P_d + C_{ST2}P(H_1)(1-P_d) + C_{ST3}(H_0)P_f + C_{ST4}P(H_0)(1-P_f) \quad (20)$$

The ultimate objective of spectrum sensing in secondary system is to maximize the system capacity.

There is a tradeoff between sensing performance and secondary system throughput. How to achieve efficient joint spectrum sensing to maximize the throughput of the secondary system is a significant problem:

$$\max_{\tau} \quad C_{ST}(\tau) \quad \text{s.t.} \quad P_{int} \le \varsigma \quad (21)$$

The above expression presents the optimization of the achievable throughput of secondary system in CRNs.

Proposition 1: For a target false alarm probability $\bar{P}_f$, $C_{ST}(\tau)$ is a strict concave function in terms of $\tau(\tau\in[\tau_{min}, T])$ if and only if Eq. 22 is satisfied:

$$P(H_1)\frac{\partial^2\left(C_{ST1}(\tau)P_d(\tau)+C_{ST2}(\tau)(1-P_d(\tau))\right)}{\partial\tau^2}+P(H_0)\bar{P}_f\frac{\partial^2 C_{ST3}(\tau)}{\partial\tau^2}<0 \quad (22)$$

For ensuring the PU interference constraint, it can be derived from Eq. 4 that $Pd(\tau)>1-\varsigma/Pm_I$ which means that:

$$\tau_{min} = \frac{M\left(Q^{-1}\left(\bar{P}_f\right)-\frac{1}{\chi}Q^{-1}\left(1-\varsigma/P_{ml}\right)\right)^2}{f_s\left(\sum_{m=1}^{M}\gamma_m\right)^2} \quad (23)$$

The proof is shown in Appendix A.

Proposition 2: For a target detection probability $\bar{P}_d C_{ST}(\tau)$, $C_{ST}(\tau)$is a strict concave function in terms of τ, if and only if Eq. 24 is satisfied:

$$\frac{\sqrt{f_s}}{2T\sqrt{2\pi\tau M}}+\frac{T-\tau}{T}\left[\frac{\sqrt{f_s}}{4\sqrt{2\pi M}\tau^{3/2}}+\frac{f_s\delta}{4\tau M\sqrt{2\pi}}\sum_{m=1}^{M}\gamma_m\right]>0 \quad (24)$$

In which:

$$\delta=\sqrt{\left(2\sum_{m=1}^{M}\gamma_m\Big/M\right)+1}Q^{-1}\left(\bar{P}_d\right)+\sqrt{\frac{\tau f_S}{M}}\sum_{m=1}^{M}\gamma_m$$

The proof is shown in Appendix B.

SIMULATION AND RESULT ANALYSIS

We present the simulation results to evaluate the joint spatial and temporal spectrum sharing mechanism in CRNs by comparing the achievable throughput of the secondary system with different spectrum sharing mechanisms. The simulation parameters are listed in Table 1.

Table 1: Simulation parameter list

Parameters	Values
Transmit power of PT: P_p (dBm)	50
Bandwidth of the specific channel: B (kHz)	200
The PT's activity: P_{H_1}	0.5
Shadowing noise: σ_W (dB)	4
Path loss factor: ρ3	
Interference threshold: κ_{max} (dB)	-80
Interference probability threshold: ς	0.01
Detection threshold of PR: r_{min} (dBm)	-30
Outage probability threshold of PR: ς	0.05
Sampling frequency: f_s (kHz)	400
Target false alarm probability: P_f	0.1
Shadowing factor: σ_X, σ_Y (dB)	0
Maximum transmit power of ST: P_{max} (dBm)	45

PT is located at the position Lp(6,6) km. All the SUs are located in a disk of radius R = 9 km with PT in the center. All the locations of M = 10 SUs for cooperative spectrum sensing are randomly generated with uniform distribution. In this study, we assume that all the cooperative spectrum sensing nodes have the same received SNR, the received SNR of the mth SU in cooperative sensing when PU signal exists is $\bar{\gamma}_m = \sigma^2_s/\sigma^2_w$ dB. D = d_{sp}-d_{cov} is denoted as the distance between SU s and the WPRP of the PT's coverage in simulation results.

Figure 3 shows the interference probability of PU caused by SU in CRNs based on joint spatial and temporal sharing with MIFTP-PS scheme. To satisfy the PU interference constraint, SU can only use the specific spectrum band with $P_d \geq 1-\varsigma/P_{mI}$. From Fig. 3, we can get that the spectrum sharing in CRNs with MIFTP-PS as spatial sensing scheme violates the constraint when d and τ are small. In CRNs based on joint spatial and temporal spectrum sharing with small d and τ, $P_{max} > P_{MIFTP-PS}(P_{mI} > P_{dI})$), the PU constraint cannot be met with MIFTP-PS.

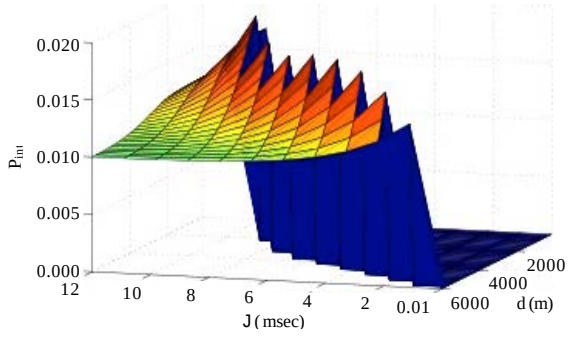

Fig. 3: Interference probability of PU in CRNs with MIFTP-PS

Figure 4 shows the interference probability and achievable throughput of secondary system with spatial spectrum sharing based on our proposed MIFTP-JSTS and MIFTP-PS, respectively, with d = 2 km. We use the interference probability and achievable throughput based on spatial spectrum sharing to evaluate these two schemes. The interference probability caused by SU is depicted with lines in red color and achievable throughput is depicted with lines in blue color in Fig. 4. We can see that although the achievable throughput with MIFTP-PS outperforms the throughput with proposed MIFTP-JSTS, P_{int} with MIFTP-PS exceeds the PU interference constraint ς while the proposed MIFTP-JSTS satisfies the PU interference constraint. With τ grows, the system performance with MIFTP-JSTS becomes closer to that with MIFTP-PS.

With given $\bar{P}_f$, the spatial spectrum hole P_{MIFTP} derived according to the MIFTP-JSTS has close relationship with temporal sensing performance. When $P_{mI} > \varsigma$, in the proposed MIFTP-JSTS, the spatial spectrum hole is constraint by $P_{dI} > 0$ which means that P_{MIFTP} have to be adjusted according to temporal detection probability P_d to satisfy the PU interference constraint.

We can see from Fig. 5 that the spatial spectrum holes in CRNs increase as d and ς. As τ grows, P_{MIFTP} with MIFTP-JSTS scheme grows and the upper bound of P_{MIFTP} can be achieved with MIFTP-PS scheme. For given $\bar{P}_f$, P_{MIFTP} does not exist with specific small ς and τ. We can get that the spatial spectrum hole increases not only with d but also the sensing duration (detection probability).

In conclusion, our proposed MIFTP-JSTS scheme is suitable for CRNs based on joint spatial and temporal spectrum sharing. The proposed MIFTP-JSTS scheme is used for spatial spectrum hole in CRNs based on joint spatial and temporal sharing in the rest of the simulation.

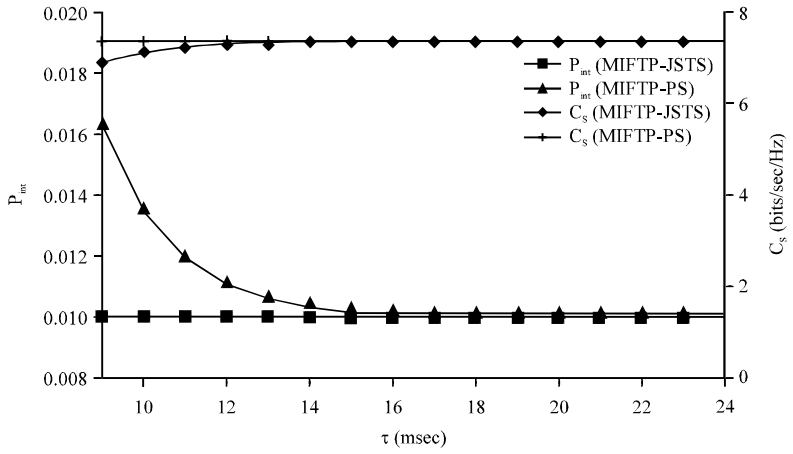

Fig. 4: Spatial spectrum sharing in CRNs

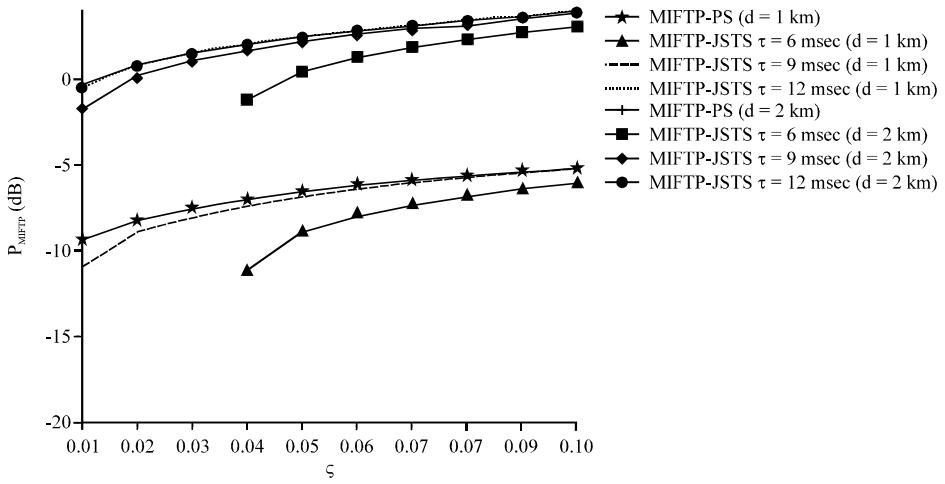

Fig. 5: Spatial spectrum hole in CRNs

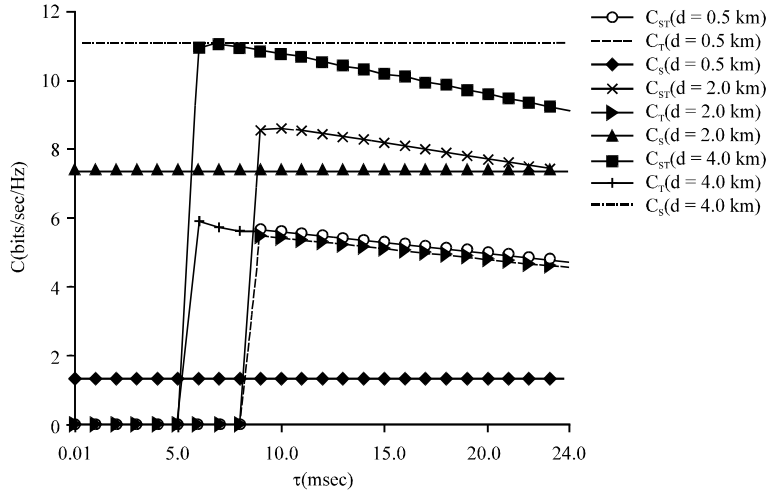

Fig. 6: Throughput of secondary system with $\bar{P}_f = 0.1$

Figure 6 shows that the throughput of the secondary system versus spectrum sensing duration in CRNs based on different spectrum sharing mechanisms.

- The achievable throughput of secondary system based on temporal spectrum sharing C_T with different d starts from different sensing duration τ_{min} to ensure the PU interference constraint ($P_d(\tau)>1-\varsigma/P_{ml}$). The threshold τ_{min} can be easily derived from Eq. 23, τ_{min} decreases with d. For $\bar{P}_f = 0.1$, the system throughput decreases monotonously with growing τ
- The achievable throughput of secondary system based on spatial spectrum sharing C_S grows as d increases. As in this study, we assume that the spatial sensing time can be ignored, C_S is independent of τ. With d large enough (d = 4 km in Fig. 7), the spatial spectrum sharing outperforms the other spectrum sharing mechanisms in terms of throughput
- The achievable throughput in secondary system based on joint spatial and temporal sharing C_{ST} grows as d increases. Spatial spectrum hole emerges only when $P_d(\tau)>1-\varsigma/P_{ml}$, i.e., $\tau \geq \tau_{min}$ which is the same as in temporal spectrum sharing. When d is smaller than d_{max} (e.g., in Fig. 7 d_{max} = 4 km), the maximum value of C_{ST} is larger than the one of C_T and C_S, in which:

$$d_{max} = \min_{d}\left(C_{ST}\left(d, \tau_{optimal}\right) == C_S\left(d\right)\right)$$

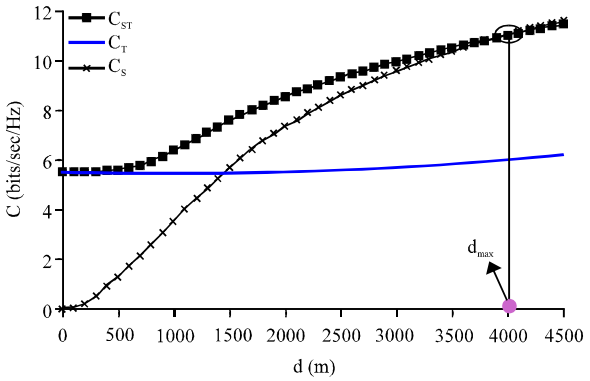

Fig. 7: Maximum throughput of secondary system with $\bar{P}_f = 0.1$

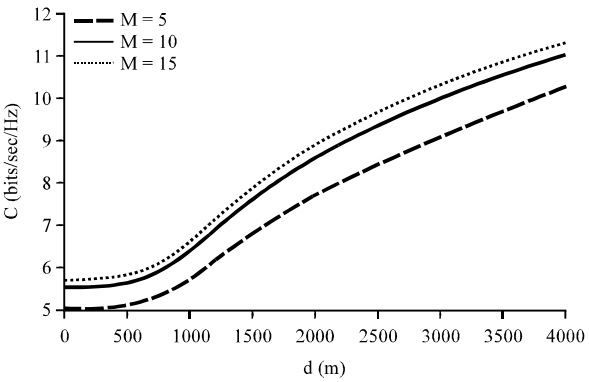

Fig. 9: Maximum throughput of secondary system based on joint spatial and temporal sharing with $\bar{P}_f = 0.1$

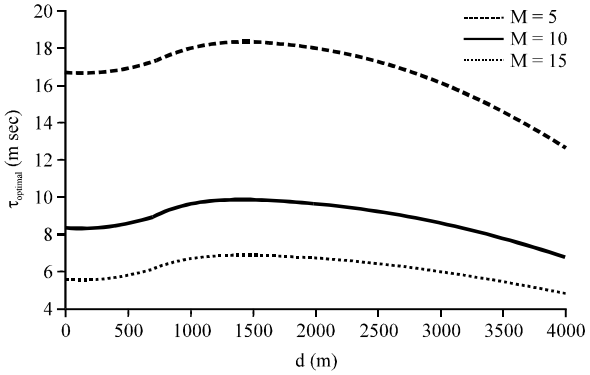

Fig. 8: Optimal sensing duration of secondary system based on joint spatial and temporal sharing with $\bar{P}_f = 0.1$

As d grows, the advantage of temporal spectrum sharing disappears and C_{ST} is smaller than C_S because the transmission time is reduced a lot for temporal sensing.

According to the proposition 1, $C_{ST}(\tau)$ is a strict concave function of τ ($\tau \geq \tau_{min}$) with the simulation parameters and given false alarm probability. Unique optimal sensing duration $\tau_{optimal}$ of secondary system exists and can be obtained by using bisection method. The corresponding maximum throughput can also be derived. In Fig. 7, we can observe that the joint spatial and temporal spectrum sharing in CRNs outperforms the spatial and temporal sharing mechanisms within a specific region with given $\bar{P}_f$, in which the region has the radius $r(d_{cov} \leq r \leq (d_{cov}+d_{max}))$.

We show the optimal sensing duration $\tau_{optimal}$ and corresponding maximized secondary system throughput in CRNs based on joint spatial and temporal sensing with different number of cooperative sensing nodes in Fig. 8 and 9, respectively. $\tau_{optimal}$ decreases as the number of sensing nodes increases and it also changes with d. The maximized throughput of secondary system increases as the number of sensing nodes increases.

Figure 10 shows that the achievable throughput of secondary system versus τ based on different spectrum sharing mechanisms with $\bar{P}_d = 0.99$. To satisfy the PU interference constraint, temporal spectrum sharing and joint spatial and temporal spectrum sharing are allowed only when $P_{mI}(d) \leq \varsigma/(1-P_d)$, with which we can get the minimum d for $\bar{P}_d$:

$$d_{minB} = g^{-1}\left[\text{erf}^{-1}\left(1-\frac{2\varsigma}{1-P_d}\right)\sigma_W\sqrt{2} + P_{max} - \kappa_{max}\right]$$

Figure 11 presents the maximized throughput of secondary system based on different spectrum sharing mechanisms with given $\bar{P}_d = 0.99$. It can be observed that as d increases, the advantage of using temporal spectrum hole in C_{ST} disappear relative to C_S, for the cost of the sensing time in temporal sensing exceeds the gain of temporal sharing.

As a result, when $d > d_{maxB}$, the spatial spectrum sharing outperforms the joint spatial and temporal spectrum sharing. Similar as the description of Fig. 6, C_{ST} is superior over C_S and C_T only in the advantage region that $d_{minB} \leq d \leq_{maxB}$, in which:

$$d_{maxB} = \min_d\left(C_{ST}\left(d, \tau_{optimal}\right) == C_S\left(d\right)\right)$$

The optimal sensing duration $\tau_{optiaml}$ and corresponding maximized secondary system throughput based on joint spatial and temporal spectrum sharing versus d with different detection probability $\bar{P}_d$ are shown in Fig. 12 and 13, respectively. $\tau_{optimal}$ decreases monotonously with d, meanwhile when the given $\bar{P}_d$ is

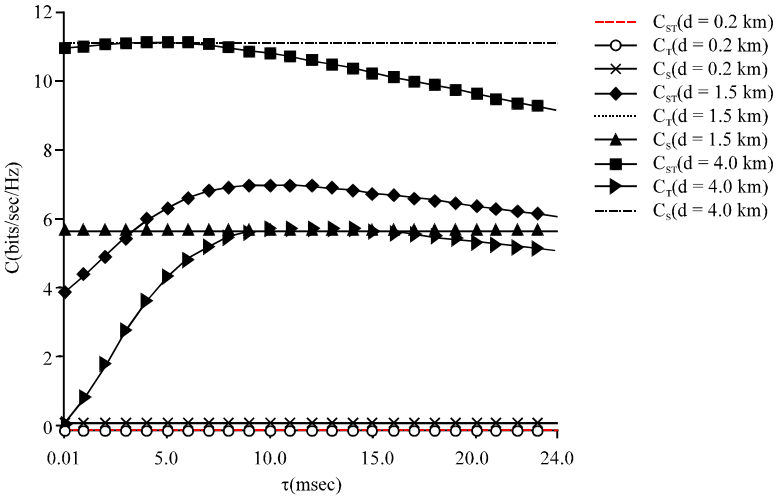

Fig. 10: Throughput of secondary system with $\bar{P}_d = 0.99$

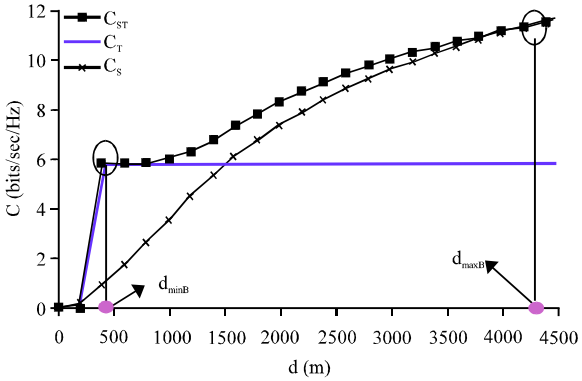

Fig. 11: Throughput of secondary system with $\bar{P}_d = 0.99$

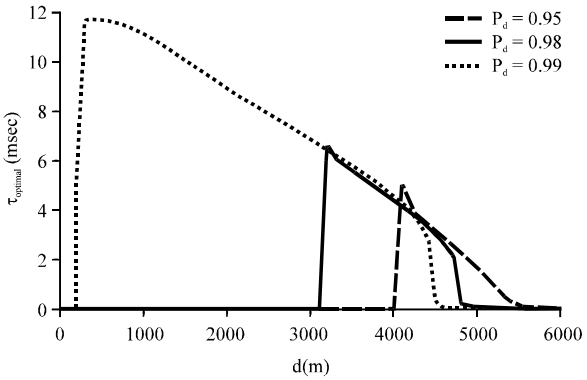

Fig. 12: Optimal sensing duration in CRNs based on joint spatial and temporal spectrum sharing

large, the joint spatial and temporal spectrum sharing can be utilized in a larger region. The corresponding maximized throughput increases monotonously with d.

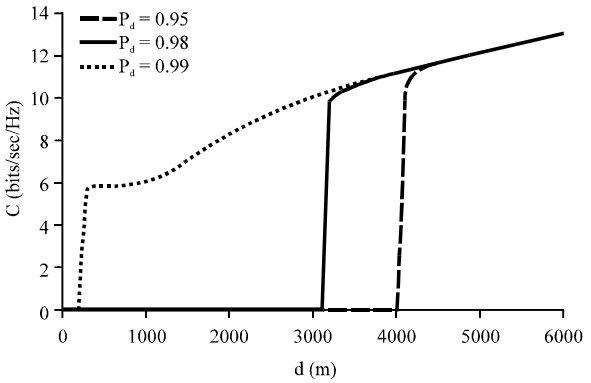

Fig. 13: Maximum throughput in CRNs based on joint spatial and temporal spectrum sharing

CONCLUSION

In this study, we propose a joint spectrum sensing scheme for CRNs based on joint spatial and temporal spectrum sharing with PU interference constraint. Also, the relationship between the spatial spectrum sensing and temporal spectrum sensing is revealed. For CRNs with specific periodical spectrum sensing, tradeoff exists between the performances of spectrum sensing and spectrum sharing. Through analysis, we can conclude that the optimal sensing duration can be derived to optimize the performance of spectrum sharing in CRNs. Meanwhile through analysis and simulation results, we can get that there are advantage regions for joint spatial and temporal spectrum sharing mechanism, where it can achieve better performance than temporal spectrum sharing and spatial spectrum sharing with given false alarm probability and detection probability, respectively.

In future research, we will study the joint spatial and temporal spectrum sharing mechanism in the situation that location and the transmit power of PU is unknown. The estimation error of PT's location, power and their influences on the sensing-throughput tradeoff will be studied.

APPENDIX

A: Proof of proposition 1:

Proof:

By differentiating τ on the two sides of Eq. 20, we can get:

$$\frac{\partial^2 C_{ST}(\tau)}{\partial \tau^2} = P(H_1)\frac{\partial^2 C_{ST1}(\tau)P_d(\tau)}{\partial \tau^2} + P(H_1)\frac{\partial^2 C_{ST2}(\tau)(1-P_d(\tau))}{\partial \tau^2} + P(H_0)\bar{P}_f\frac{\partial^2 C_{ST3}(\tau)}{\partial \tau^2} + P(H_0)(1-\bar{P}_f)\frac{\partial^2 C_{ST4}(\tau)}{\partial \tau^2} \quad \text{(A-1)}$$

$$\frac{\partial^2 C_{ST1}P_d(\tau)}{\partial \tau^2} = \left(\frac{a_4 + a_3\cdot(T-\tau) - 2\cdot a_1}{T}\right)P_d(\tau) + \left(\frac{2\cdot a_1\cdot(T-\tau) - 2\cdot a_2}{T}\right)\frac{\partial P_d(\tau)}{\partial \tau} + \frac{(T-\tau)\cdot a_2}{T}\frac{\partial^2 P_d(\tau)}{\partial \tau^2} \quad \text{(A-2)}$$

$$\frac{\partial^2 C_{ST2}(\tau)(1-P_d(\tau))}{\partial \tau^2} = \left(\frac{\log(1+P_{max}\lambda_2)}{T} + \frac{\lambda_2}{T(1+P_{max}\lambda_2)}\right)\frac{\partial P_d(\tau)}{\partial \tau} - \frac{\lambda_2(T-\tau)}{T(1+P_{max}\lambda_2)}\frac{\partial^2 P_d(\tau)}{\partial \tau^2} \quad \text{(A-3)}$$

In which:

$$a_1 = B\cdot E\left\{\frac{\lambda_2}{1+\lambda_2 P_{MIFTP}(\tau)}\frac{\partial P_{MIFTP}(\tau)}{\partial \tau}\right\}$$

$$a_2 = B\cdot E\left\{\log_2\left(1+P_{MIFTP}(\tau)\lambda_2\right)\right\}$$

$$a_3 = B\cdot E\left\{\frac{\lambda_2}{1+\lambda_2 P_{MIFTP}(\tau)}\frac{\partial^2 P_{MIFTP}(\tau)}{\partial \tau^2}\right\}$$

$$a_4 = B\cdot E\left\{\frac{\lambda_2^2}{\left(1+\lambda_2 P_{MIFTP}(\tau)\right)^2}\left(\frac{\partial P_{MIFTP}(\tau)}{\partial \tau}\right)^2\right\}$$

$$\lambda_2 = \frac{\left(\frac{d_0}{D_{ii}}\right)^n e^X}{P_p\left(\frac{d_0}{D_{ii}}\right)^n e^Y + N_0 B}$$

$$\frac{\partial^2 C_{ST3}(\tau)}{\partial \tau^2} = \left(-\frac{2}{T}\right)B\cdot E\left\{b\frac{\partial P_{MIFTP}(\tau)}{\partial \tau}\right\} + \frac{T-\tau}{T}B\cdot E\left\{b^2\left(\frac{\partial P_{MIFTP}(\tau)}{\partial \tau}\right)^2 + b\frac{\partial^2 P_{MIFTP}(\tau)}{\partial \tau^2}\right\} \quad \text{(A-4)}$$

In which:

$$b = \frac{\lambda_1}{1+\lambda_1 P_{MIFTP}(\tau)},\ \lambda_1 = \frac{(d_0/D_{ii})^n e^X}{N_0 B}$$

$$\frac{\partial^2 C_{ST4}(\tau)}{\partial \tau^2} = 0 \quad \text{(A-5)}$$

If and only if Eq. 22 is satisfied, then with given $\bar{P}_f$, $C_{ST}(\tau)$ is a strict concave function in terms of τ in the range $\tau_{min} \le \tau \le T$.

B: Proof of proposition 2:

Proof:

$$\frac{\partial^2 C_{ST}(\tau)}{\partial \tau^2} = \frac{1}{T}P(H_0)(C_d - C_c)\frac{\partial P_f(\tau)}{\partial \tau} + \frac{T-\tau}{T}P(H_0)(C_c - C_d)\frac{\partial^2 P_f(\tau)}{\partial \tau^2} \quad \text{(B-1)}$$

In which:

$$C_c = B\cdot E\left\{\log_2\left(1+\frac{P_{MIFTP}\left(\frac{d_0}{D_{ii}}\right)^n e^X}{N_0 B}\right)\right\} \quad \text{(B-2)}$$

$$C_d = B\cdot E\left\{\log_2\left(1+\frac{P_{max}\left(\frac{d_0}{D_{ii}}\right)^n e^X}{N_0 B}\right)\right\} \quad \text{(B-3)}$$

$$\frac{\partial P_f(\tau)}{\partial \tau} = -\frac{\sqrt{f_s}}{2\sqrt{2\pi\tau M}}\sum_{m=1}^{M}\gamma_m \exp\left(-\frac{\delta^2}{2}\right) \quad \text{(B-4)}$$

$$\frac{\partial^2 P_f(\tau)}{\partial \tau^2} = \frac{\sqrt{f_s}}{4\sqrt{2\pi M}\tau^{3/2}}\sum_{m=1}^{M}\gamma_m \exp\left(-\frac{\delta^2}{2}\right) + \frac{f_s\delta}{4\tau M\sqrt{2\pi}}\left(\sum_{m=1}^{M}\gamma_m\right)^2 \exp\left(-\frac{\delta^2}{2}\right) \quad \text{(B-5)}$$

In which:

$$\delta = \frac{1}{\chi}Q^{-1}(\bar{P}_d) + \sqrt{\frac{\tau f_s}{M}}\sum_{m=1}^{M}\gamma_m$$

As known $P_{MIFTP} < P_{max}$, we can get that $C_d > C_c$. By substituting Eq. B-4 and Eq. B-5 into Eq. B-3, we can get that if and only if Eq. 24 is satisfied, then $C_{ST}(\tau)$ is a strict concave function of τ with given $\bar{P}_f$.

REFERENCES

Chen, P.P., Q.Y. Zhang, J. Yu, Y.L. Zhang and B. Cao, 2013. Sensing-throughput tradeoff in joint spatial-temporal sensing based cognitive radio networks. Proceedings of the International Conference on Communications in China, August 12-14, 2013, Xi'an, China, pp: 727-732.

Do, T. and B.L. Mark, 2010. Joint spatial-temporal spectrum sensing for cognitive radio networks. IEEE Trans. Veh. Technol., 59: 3480-3490.

FCC, 2002. Spectrum policy task force report. Federal Communications Commission, ET Docket No. 02-135, November 2002. http://hraunfoss.fcc.gov/edocs_public/attachmatch/DOC-228542A1.pdf

Ghasemi, A. and E.S. Sousa, 2008. Spectrum sensing in cognitive radio networks: Requirements, challenges and design trade-offs. IEEE Commun. Mag., 46: 32-39.

Islam, M.H., C.L. Koh, S.W. Oh, X. Qing and Y.Y. Lai *et al.*, 2008. Spectrum survey in Singapore: Occupancy measurements and analyses. Proceedings of the 3rd International Conference on Cognitive Radio Oriented Wireless Networks and Communications, May 15-17, 2008, Singapore, pp: 1-7.

Kay, S.M., 1998. Fundamentals of Statistical Signal Processing: Detection Theory. Vol. 2, Prentice-Hall PTR, Englewood Cliffs, NJ., ISBN: 9780135041352, Pages: 672.

Liang, Y.C., Y. Zeng, E.C.Y. Peh and A.T. Hoang, 2008. Sensing throughput tradeoff for cognitive radio networks. IEEE Trans. Wireless Commun., 7: 1326-1337.

Mark, B.L. and A.O. Nasif, 2009. Estimation of maximum interference-free power level for opportunistic spectrum access. IEEE Trans. Wireless Commun., 8: 2505-2513.

Min, A.W., X. Zhang and K.G. Shin, 2010. Spatio-temporal fusion for small-scale primary detection in cognitive radio networks. Proceedings of the IEEE 29th Conference on Computer Communications, March 15-19, 2010, San Diego, CA., pp: 381-385.

Mitola III, J., 1999. Cognitive radio for flexible mobile multimedia communications. Mobile Networks Appl., 6: 435-441.

NTIA, 2003. US frequency allocation chart (the radio spectrum). National Telecommunications and Information Administration, October 2003. http://www.ntia.doc.gov/files/ntia/publications/2003-allochrt.pdf

Sahai, A., N. Hoven, S.M. Mishra and R. Tandra, 2006. Fundamental tradeoffs in robust spectrum sensing for opportunistic frequency reuse. IEEE J. Select. Areas Commun., 1: 1-75.

Taricco, G., 2011. Optimization of linear cooperative spectrum sensing for cognitive radio networks. IEEE J. Selected Topics Signal Process., 5: 77-86.

Zou, Q., S. Zheng and A.H. Sayed, 2010. Cooperative sensing via sequential detection. IEEE Trans. Signal Process., 58: 6266-6283.